# Absence of radius and ulna in mice lacking *hoxa-11* and *hoxd-11*

**Allan Peter Davis*, David P. Witte†, Hsiu M. Hsieh-Li†, S. Steven Potter† & Mario R. Capecchi*‡**

* Howard Hughes Medical Institute, Department of Human Genetics, University of Utah School of Medicine, Salt Lake City, Utah 84112, USA
† Division of Basic Science Research and Pathology, Children's Hospital Research Foundation and Department of Pediatrics, University of Cincinnati College of Medicine, Cincinnati, Ohio 45229, USA
‡ To whom correspondence should be addressed

**MICE with targeted disruptions[1] in *Hox* genes have been generated to evaluate the role of the *Hox* complex in determining the mammalian body plan. This complex of 38 genes encodes transcription factors that specify regional information along the embryonic axes. Early in vertebrate evolution an ancestral complex shared with invertebrates was duplicated twice to give rise to the four linkage groups (Hox A, B, C and D)[2,3]. As a consequence, corresponding genes on the separate linkage groups, called paralogues, are most closely related to each other. Based on sequence similarities, the *Hox* genes have been subdivided into 13 paralogous groups. The five most 5′ groups (*Hox* 9–13) pattern the posterior region of the vertebrate embryo and the appendicular skeleton[4–18]. Mice with individual mutations in the paralogous genes *hoxa-11* and *hoxd-11* have been described[15–18]. By breeding these two strains together we have generated double mutants which have dramatic phenotypes not apparent in mice homozygous for the individual mutations. The radius and the ulna of the forelimb are almost entirely eliminated, the axial skeleton shows homeotic transformations, and there are severe kidney defects not present in either single mutant. The limb and axial phenotypes are quantitative: as more mutant alleles are added to the genotype, the phenotype becomes progressively more severe. The appendicular skeleton defects suggest that paralogous *Hox* genes function together to specify limb outgrowth and patterning along the proximodistal axis.**

For simplicity, we use 'A' (wild-type allele) and 'a' (mutant allele) to designate the *hoxa-11* genotype, and similarly 'D' and 'd' for *hoxd-11*. Compound heterozygotes (Aa; Dd) were crossed to each other to generate all nine genetic states. Four (aa; dd) adults were weaned from a total of 313 progeny. This is fewer than the 20 expected; most double mutants suffer perinatal death as a consequence of kidney dysfunction (see below). All other genotypes occurred in the expected Mendelian ratios.

The vertebrate forelimb is divided into three zones: the stylopod (humerus), zeugopod (radius and ulna), and autopod (carpals, metacarpals and phalanges) (Fig. 1*a*). The hindlimb is similarly arranged. All four limbs of the double mutants are severely affected. Synergistic effects of *hoxa-11* and *hoxd-11* are dramatic in the forelimb zeugopod wherein individual mutant homozygotes (aa; DD) and (AA; dd) show subtle malformations of the zeugopod (Fig. 1*b*, *c*), but, remarkably, the radius and ulna are almost entirely absent from double-mutant limbs (Fig. 1*d*). These extraordinary malformations result in a paw that is rotated 90° off its normal axis.

There are similar effects in the autopod. The wrist contains seven bones: three proximal carpals (pisiform, triangular and navicular lunate) and four distal carpals (d1–d4). In (aa; DD) and (AA; dd) forelimbs the proximal carpal bones are fused together[15–17]. Although individual heterozygotes never show this defect, compound heterozygotes (Aa; Dd) do (Table 1). This suggests that any two mutant alleles (either both from *hoxa-11* or *hoxd-11*, or one from each locus) will cause carpal fusions. Genotypes (Aa; dd) and (aa; Dd), with three mutant alleles, have more severe defects of the proximal carpal bones in which the triangular and pisiform bones are grossly malformed, and the navicular lunate is slightly deformed (results not shown).

TABLE 1 Axial and carpal bone phenotypes of (*hoxa-11*; *hoxd-11*) mice

| | Axial column phenotypes | | | Carpal bone phenotypes | | | | |
|---|---|---|---|---|---|---|---|---|
| | | | | | | Carpal bone fusions¶ | | |
| Genotype* | Phenotype† | Frequency (%)‡ | Comments§ | Genotype | Wild-type (%) | NL-T | T-P | NL-T-P |
| (AA; DD) | T13:L6 | 100 | wild-type | (AA; DD) | 100 | | | |
| (Aa; DD) | T13:L6<br>T12:L7 | 50<br>50 | wild-type<br>PHT | (Aa; DD) | 100 | | | |
| (aa; DD) | T12:L8<br>T12:L7:AL/S | 50<br>50 | PHT and AHT<br>PHT and AHT | (aa; DD) | 33 | 17% | 50% | |
| (AA; Dd) | T13:L6 | 100 | wild-type | (AA; Dd) | 100 | | | |
| (AA; dd) | T13:L7<br>T13:L6:AL/S | 50<br>50 | AHT<br>AHT | (AA; dd) | | 17% | 17% | 67% |
| (Aa; Dd) | T12:L7<br>T13:L7<br>T12:AT/L:L6<br>T12:AT/L:L7 | 33<br>33<br>17<br>17 | PHT<br>AHT<br>PHT<br>PHT and AHT | (Aa; Dd) | 17 | 17% | 33% | 33% |
| (Aa; dd) and (aa; Dd)‖ | T12:L8<br>T13:L7 | 67<br>33 | PHT and AHT<br>AHT | | | | | |
| (aa; dd) | T12:L9<br>T12:L8:AL/S | 75<br>25 | PHT and AHT<br>PHT and AHT | | | | | |

* A, *hoxa-11* wild-type allele; a, mutant allele; D, *hoxd-11* wild-type allele; d, mutant allele.
† T13:L6, wild-type pattern with 13 thoracics (T) followed by 6 lumbars (L). AL/S is an asymmetric vertebra: half is lumbar-like, half is sacral-like. AT/L is an asymmetric vertebra: half is thoracic-like, half is lumbar-like.
‡ Examined six animals for each genotype, except for (aa; dd) where only four were available.
§ PHT (posterior homeotic transformation); AHT (anterior homeotic transformation).
‖ (Aa; dd) and (aa; Dd) data combined.
¶ Percentage of animals either showing a wild-type pattern of carpals (none fused) or a fusion between the navicular lunate (NL), triangular (T), and pisiform (P) carpal bones.

The distal carpals in these animals appear normal. With the addition of a fourth mutant allele, the autopod of the mouse is even more dramatically altered. All of the proximal carpal bones are affected: the pisiform is missing, the triangular is also either absent or is fused to the distal carpals, and the navicular lunate is deformed (Fig. 2*a*, *b*). The metacarpals are reduced in length, especially in digits II, III and V. In addition, digits I, II and III curve preaxially and are 'fused' together by the overlaying skin, perhaps owing to a failure of normally occurring cell death between the digits. The phalangeal bones P2 and P1 of digit III are often fused, and P2 is missing from digits II and V (Fig. 2*a*–*d*).

The zeugopodal phenotype is evident at E13.5 when the radius and ulna branch off from the humerus (Fig. 2*e*, *f*). At this stage the (aa; dd) zeugopod is already shorter than the wild type. In addition, the autopod condensations are altered. The wild-type autopod has initiated a full complement of digits, but condensa-

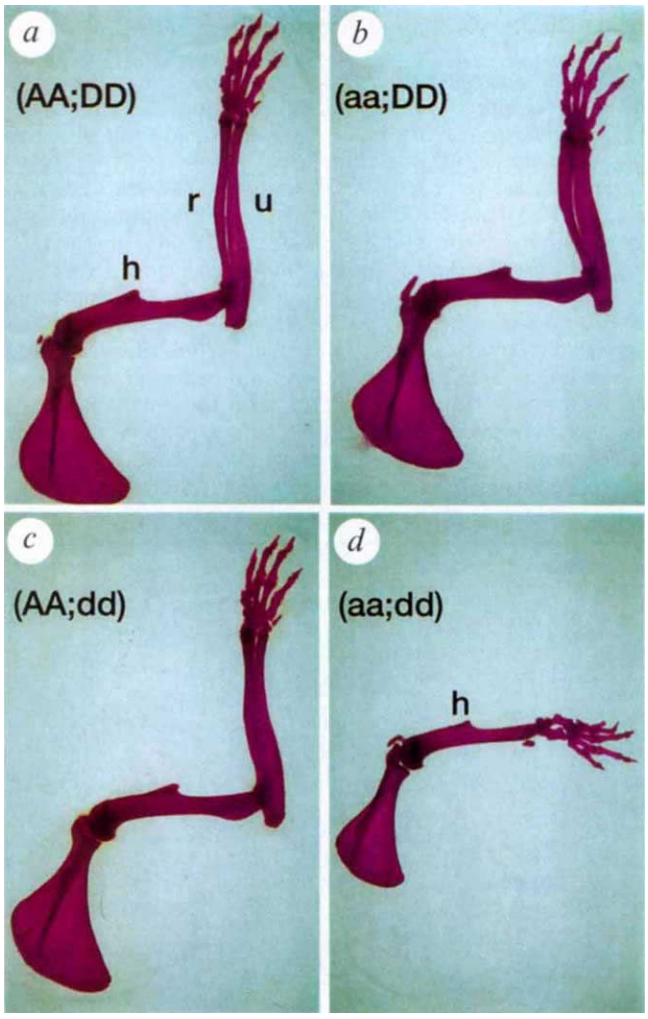


FIG. 1 Loss of the radius and ulna in the double-mutant mouse. Dorsal view of the right forelimbs from adult mouse skeleton preparations. *a*, Wild-type mouse (AA; DD) with a normal humerus (h), radius (r), and ulna (u). *b*, *Hoxa-11* mutant (aa; DD) with a slightly thicker and shorter zeugopod. *c*, *Hoxd-11* mutant (AA; dd) with subtle limb defects in the zeugopod and autopod[16]. *d*, The double mutant (aa; dd) showing an unexpected and dramatic reduction of the radius and ulna. The forepaw is also malformed and rotated 90° compared with wild type. Four (aa; dd) mice survived to adulthood and were examined. All four showed complete penetrance and expressivity of the limb phenotype.
METHODS. All animals were genotyped by Southern blot analysis of tail DNA, and adult skeleton preparations were stained with Alizarin red as described[15,16].

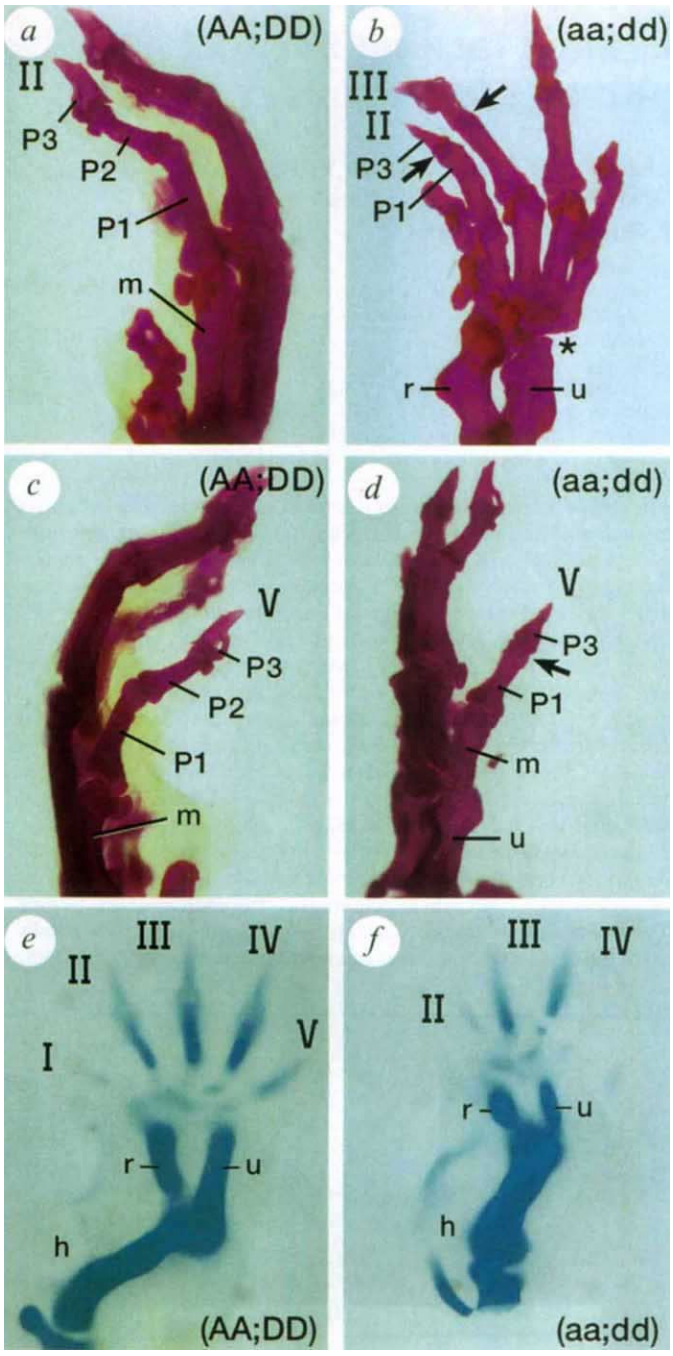


FIG. 2 Autopod defects in the double-mutant mouse. *a*, Wild-type (AA; DD) digit II with normal phalanges (P3, P2, P1) and metacarpal (m). *b*, The double mutant (aa; dd) shows several defects in the autopod. P2 is missing from digit II and is fused to P1 in digit III (arrows). The pisiform and triangular carpal bones are missing (star) and the navicular lunate is deformed. A small vestige of the radius (r) and ulna (u) remains. Digits I, II and III curve preaxially. Digit IV appears relatively normal. *c*, Wild-type (AA; DD) digit V with normal phalanges and metacarpal. *d*, The double mutant (aa; dd) digit V lacks P2 (arrow). *e*, Cartilage condensations in the developing right forelimb of wild-type mouse (AA; DD) at embryonic stage E13.5, showing the humerus (h), radius (r) and ulna (u) with digits I–V all initiated. *f*, Zeugopod defect is already evident in the double mutant (aa; dd) with a reduced radius and ulna. Only digits IV, III and part of II have started to condense. The scapula became detached from the mutant limb and is not shown.
METHODS. Embryos were collected, genotyped and stained with Alcian blue as described[19].

tions in the double mutant (aa; dd) paw are delayed with only digits IV, III and part of II formed.

Intermediate genotypes with three mutant alleles produce intermediate phenotypes in the radius and ulna. These animals have a reduction in the length of the zeugopod as well as a substantial bowing of the radius (Fig. 3*a–c*). As predicted from a quantitative phenotype, (Aa; dd) and (aa; Dd) limbs cannot be distinguished from each other by inspection. The hindlimbs of the double mutant are also affected (Fig. 3*d*, *e*). In double-mutant mice, the fibula is thickened and flared at its distal end and is never fused with the tibia, all in contrast to wild-type mice. Most noticeable, however, is the absence of the proximal tarsal bones (the talus and calcaneus/processus trochlearis) from double-mutant mice. This forces the tibia and fibula to join the foot at the mid-tarsals. Interestingly, the hindlimb phenotype is not quantitative with respect to the number of mutant alleles because intermediate genotypes (aa; Dd) and (Aa; dd) do not have intermediate phenotypes.

The normal mouse axial skeleton is characterized by 7 cervical (C1–7), 13 thoracic (T1–13), 6 lumbar (L1–6), 4 sacral (S1–4), and a variable number of caudal vertebrae. The transverse processes on S1–3 fuse to form the sacrum. Table 1 shows a summary of the vertebral phenotypes for mice generated from intercrosses of compound heterozygotes. Both the (aa; DD) and the (AA; dd) mutant mice show an apparent homeotic transformation of the first sacral vertebra towards a lumbar vertebra (S1→L)[15–17]. Half of the compound heterozygotes (Aa; Dd) show this same transformation, a phenotype never observed in either of the individual heterozygotes (Aa; DD) and (AA; Dd). Again, this quantitative phenotype suggests that only two mutant alleles (either of *hoxa-11*, or *hoxd-11*, or one from each locus) are necessary to induce this homeosis. The double mutant (aa; dd) has nine lumber vertebrae (Table 1). These can be accounted for by both a posterior homeotic transformation (T13→L1) and a double anterior homeotic transformation (S1, S2→L8, L9). In addition, the sacral vertebrae do not fuse to form a sacrum, and in some cases the second sacral vertebra and one caudal vertebra are deleted.

*hoxa-11* and *hoxd-11* are expressed in the primitive blastemal cells that populate the nephrogenic zone of the developing kidney (ref. 18, and S.S.P., unpublished results). Whereas mice mutant for either *hoxa-11* or *hoxd-11* have normal kidneys[15,16], double mutants (aa; dd) suffer renal malformations that generally result in perinatal death (Fig. 4*a*, *b*). Some double-mutant mice are born lacking one or both kidneys. Newborn (aa; dd) mice with kidneys show severe renal hypoplasia (Fig. 4*b*), with poorly developed cortex and medulla and little or no nephrogenic activity in the subcapsular region (Fig. 4*c*, *d*). The rare adult (aa; dd) kidney has a thick wall of cortical tissue and poorly developed renal papillae. The renal tubules present are well developed and the glomerulae, although severely reduced in number, show only mild compensatory hypertrophy (results not shown). There were no abnormalities in the lower renal tract to suggest urinary obstruction. With rare exceptions, one wild-type allele of either *hoxa-11* or *hoxd-11* was sufficient for normal kidney development. Urogenital malformations also include homeotic transformation of the vas deferens towards an epididymis. This is apparent at the gross level, with the vas deferens of (aa; dd) mice being smaller in diameter and more coiled than normal (Fig. 4*e*, *f*), and also evident at the histological level, with the mutant vas deferens showing reduction of the muscle layer, lack of convolution of the epithelial layer, and an epididymis-like epithelial cell morphology with nuclei positioned peripherally instead of centrally (Fig. 4*g–i*).

We expect that quantitative interactions between *Hox* genes will be the rule rather than the exception. Previously we demon-

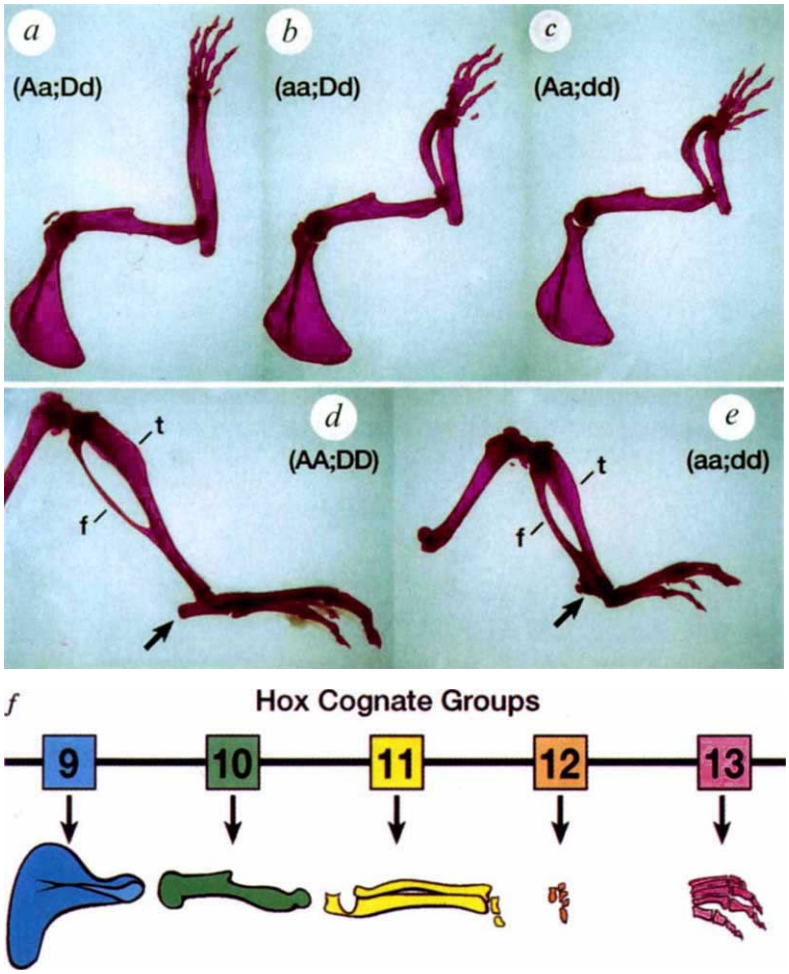


FIG. 3 Genetic quantification and synergy in the limb phenotypes. *a*, Compound heterozygote (Aa; Dd) forelimb. *b*, *c*, Mice with three mutant alleles (*b*, (aa; Dd) and *c*, (Aa; dd)) show intermediate phenotypes with a shortening and thickening of the zeugopod and with a substantial bowing of the radius. *d*, Wild-type (AA; DD) right hindlimb with normal tibia (t) and fibula (f) and proximal tarsal bones present (arrow). *e*, Double mutant (aa; dd) has malformed tibia and fibula that are slightly thicker and never fuse together, the proximal tarsal bones are also missing (arrow). *f*, A model for the role of *Hox* genes in limb development. The Hox cognate groups 9–13 represent the combined paralogous genes of the *Hox* loci and are drawn in the 3′ to 5′ direction. We propose that the cognate genes work in union to specify limb bone formation in the proximal to distal direction (left to right). In the double-mutant mouse (aa; dd), both *hoxa-11* and *hoxd-11* are mutated; this results in the loss of the radius, ulna and proximal carpals (yellow coded bones). In addition to these paralogous interactions, *Hox* genes in the same linkage group or across groups may also interact during limb development.

strated that the two paralogues *hoxa-3* and *hoxd-3* interact quantitatively to specify the craniocervical joint[19] and that *hoxb-5* and *hoxb-6* function together to specify cervical and thoracic vertebrae[20]. Here we describe quantitative, synergistic genetic interactions between *hoxa-11* and *hoxd-11*. In the vertebral column and carpal bones, compound heterozygotes have phenotypes similar to mice homozygous for mutations in either *hoxa-11* or *hoxd-11*. The quantitative effect is further revealed in animals with three mutant alleles: forelimbs in (aa; Dd) and (Aa; dd) mice show more severe defects in the zeugopod and autopod than are found in animals with only two mutant alleles. Synergy is seen in the axial column, limbs, kidneys and vas deferens, where phenotypes of the double mutant (aa; dd) are more pronounced than the sum of the phenotypes seen in the individual mutant homozygotes.

Limb bones are formed from prechondrogenic condensations that segment and bifurcate along the proximodistal axis to create the long bones (humerus, then radius and ulna). This is followed by proximodistal and anteroposterior condensations to generate the carpals, metacarpals and digits[21,22]. Mice with targeted disruptions of either *hoxa-11* or *hoxd-11* show regional malformations in the shape, length and segmentations of bones in the zeugopod and autopod[15–17]. These defects do not resemble homeotic transformations, but rather perturbations in the growth of the cells contributing to the prechondrogenic condensations. Further, the defects are not polarized with respect to the anteroposterior axis. It is therefore surprising that in double mutants the radius and ulna are almost entirely eliminated. In addition, the phenotype of the (aa; dd) autopod is strongly polarized. The more posterior proximal carpals are severely affected, whereas the distal carpals seem normal. The digits are also malformed. Digit IV seems to be normal, but the severity in phenotypes increases through digit III (a fusion between P2 and P1) to a maximum in digits II and V (both lacking P2). This phenotypic progression parallels the developmental 'limb plan' that proposes a basic axis of development that proceeds through the humerus, the ulna, and then anteriorly through the wrist such that the anterior distal carpals are the last to be made[21,23]. These wrist cartilages then branch to form the digits in a specific temporal sequence: digits IV and III are the first to be made, followed by digits I, II and V[21].

The limb phenotype of the double mutants (aa; dd) suggests that these two genes function together to specify the radius and the ulna. *Hox* genes are activated in the limb bud in a temporal sequence with the 3′ genes expressed first and the 5′ genes last, creating a transcriptional cascade of *Hox-9, -10, -11, -12* and then *-13* (ref. 11). We propose that it is the activation order and the interaction of the paralogues that specify patterns of prechondrogenic condensations along the proximodistal axis (Fig. 3*f*). Their role may be achieved by regulating cell proliferation and/or survival as well as specifying cell identity (that is, the number of chondrocytes). Thus the *Hox* group 11 genes would specify the zeugopod. In the double mutant mouse, *hoxa-11* and *hoxd-11* gene products are both absent, and this region is made as a rudiment at best. But once this crisis period is over, the *Hox* group 12 genes would be activated and limb develop-

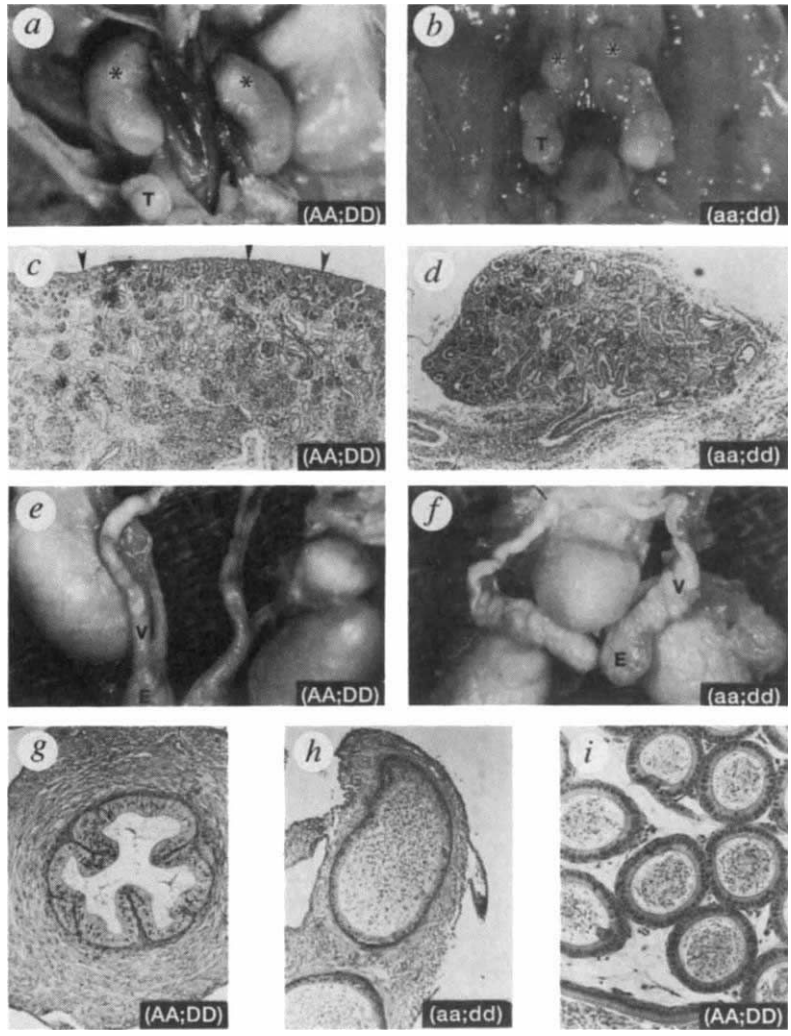


FIG. 4 Urogenital defects in the double-mutant mouse. *a*, Urinary tract of a wild-type newborn. The kidneys are indicated by the asterisk just above the testes (T). *b*, Urinary tract in the (aa; dd) mutant. The kidneys are extremely hypoplastic but the testes (T) are normal in size. *c*, Histology of wild-type kidney. Note the uniform zone of active nephrogenesis just beneath the renal capsule (arrowheads). The immature tubules and primitive glomeruli just beneath the capsule are separated by nests of undifferentiated blastemal cells. *d*, Histology of the (aa; dd) mutant kidney. In contrast with the wild-type kidney, the entire mutant kidney is easily seen at the same magnification. Although the tubules and glomeruli present are well developed, there is a decrease in total number of nephrons, with little nephrogenesis in the subcapsular zone. *e*, Dissected male reproductive tract from a wild-type mouse. There is a sharp transition from the epididymis (E) to the vas deferens (V). The vas deferens is a thick cord with a relatively straight configuration. *f*, Reproductive tract from the (aa; dd) mutant. The transition from the epididymis (E) to the vas deferens (V) is more obscure. The proximal vas deferens has a highly coiled configuration. *g*, Histology of the wild-type vas deferens. The epithelial layer has prominent folds and the lining cells have a large amount of cytoplasm with their nuclei in the middle or apical aspect of the cells. There is also a well developed smooth muscle layer in the wall of the vas deferens. *h*, Histology of the (aa; dd) mutant vas deferens. The epithelial lining is simple with no folds, and the cells are columnar and have nuclei with a uniform distribution in the basal aspects of the cells. The layer of smooth muscle cells in the wall is greatly reduced. *i*, Histology of a normal epididymis. The tubules are lined by a simple layer of columnar cells with nuclei that are uniformly arranged in the basal aspects of the epithelial cells. Note the close resemblance of this epithelial lining to that of the vas deferens from the double-mutant mice in *h*.
METHODS. Tissue samples were fixed in Bouin's solution and processed as described[18]. Sections were stained with haematoxylin and eosin.

ment resumed. In this sense, it is important to note that after the zeugopodal defect, limb development does proceed in the double-mutant mouse, albeit with some dysmorphology. But clearly the autopod is less affected than the zeugopod. The autopodal phenotypes distal to the major zeugopodal defects are likely to be the result of a coupling between proximodistal and anteroposterior patterning[24–28]. This coupling may be genetic, with group 11 genes directly influencing the timing of activation of group 12 and group 13 genes. Alternatively, morphological coupling may account for these defects. The elimination of both *hoxa-11* and *hoxd-11* gene products may reduce the overall mesenchymal cell population available to form the zeugopod and posterior carpals. A deficiency of cells may also alter the timing ('heterochrony') of formation of the rest of the limb. The second crisis would therefore be revealed at the end of autopod formation, when cartilaginous elements are competing to recruit the few remaining cells. This heterochrony would explain the delay in digit condensation seen during embryogenesis of the double mutant and account for the more severe phalangeal defects seen in digits II and V, which are the last elements formed in the last digits specified.

It is interesting that in the double mutants the forelimbs are more affected than the hindlimbs. Also, whereas (aa; Dd) and (Aa; dd) mice show an intermediate forelimb phenotype, the presence of a third mutant allele does not alter the hindlimb phenotype beyond what is seen in (aa; DD) or (AA; dd) mice. These differences may be a consequence of a third paralogue, *hoxc-11*, which is expressed more strongly in the hindlimbs[29] and could provide a compensatory function. This hypothesis would predict that in (*hoxa-11*, *hoxc-11*, *hoxd-11*) triple mutants, the tibia and fibula would be completely eliminated and show quantitative dependence on the dosage of mutant alleles. Also, the last vestige of the forelimb radius and ulna observed in the double mutant would be predicted to be absent.

Our model is supported by the *hoxd-13* mutant mouse in which the mutant limb phenotype is restricted to the autopod[13], and predicts that in a (*hoxa-13*, *hoxd-13*) double mutant the forepaw should be absent. *hoxd-12* has no paralogue in the *Hox A* family and may therefore act on its own (or in conjunction with *hoxc-12*) to influence formation of the carpals and tarsals. Alternatively, *hoxd-12* may recruit its closest *Hox A* paralogue (*hoxa-11* or *hoxa-13*) to help specify this region. Single-mutant mice for *hoxa-10*, *hoxc-10* and *hoxd-10* should show subtle defects in the humerus and femur, but double and triple mutants should affect strongly the entire stylopod and initiate a cascade of less severe phenotypes downstream through the zeugopod and autopod. Consistent with the model, individual *hoxd-10* and *hoxc-10* mutant homozygotes show mild malformations of the humerus and femur (E. M. Carpenter, J. M. Goddard and M.R.C., unpublished results; S. L. Hostikka and M.R.C., unpublished results). From this model, the appendicular ground state would be achieved in an animal lacking all of the *Hox* 10–13 cognate genes. This should be a limbless mouse. □

Received 10 April; accepted 18 May 1995.


1. Capecchi, M. R. *Scient Am.* **270,** 54–61 (1994).
2. Holland, P. W. H., Garcia-Fernandez, J., Williams, N. A. & Sidow, A. *Development* (Suppl.), 125–133 (1994).
3. Ruddle, F. H. *et al. A. Rev. Genet.* **28,** 423–442 (1994).
4. Dollé, P., Izpisúa-Belmonte, J.-C., Falkenstein, H., Renucci, A. & Duboule, D. *Nature* **342,** 767–772 (1989).
5. Dollé, P., Izpisúa-Belmonte, J.-C., Brown, J. M., Tickle, C. & Duboule, D. *Genes Dev.* **5,** 1767–1776 (1991).
6. Duboule, D. *Curr. Opin. Genet. Dev.* **1,** 211–216 (1991).
7. Izpisúa-Belmonte, J.-C., Tickle, C., Dollé, P., Wolpert, L. & Duboule, D. *Nature* **350,** 585–589 (1991).
8. Izpisúa-Belmonte, J.-C., Falkenstein, H., Dollé, P., Renucci, A. & Duboule, D. *EMBO J.* **10,** 2279–2289 (1991).
9. Yokouchi, Y., Sasaki, H. & Kuroiwa, A. *Nature* **353,** 443–445 (1991).
10. Duboule, D. *BioEssays* **14,** 375–384 (1992).
11. Izpisúa-Belmonte, J.-C. & Duboule, D. *Devl Biol.* **152,** 26–36 (1992).
12. Morgan, B. A., Izpisúa-Belmonte, J.-C., Duboule, D. & Tabin, C. *Nature* **358,** 236–239 (1992).
13. Dollé, P. *et al. Cell* **75,** 431–441 (1993).
14. Haack, H. & Gruss, P. *Devl Biol.* **157,** 410–422 (1993).
15. Small, K. M. & Potter, S. S. *Genes Dev.* **7,** 2318–2328 (1993).
16. Davis, A. P. & Capecchi, M. R. *Development* **120,** 2187–2198 (1994).
17. Favier, B., Le Meur, M., Chambon, P. & Dollé, P. *Proc. natn. Acad. Sci. U.S.A.* **92,** 310–314 (1994).
18. Li, H. M. H. *et al. Development* **121,** 1373–1385 (1995).
19. Condie, B. G. & Capecchi, M. R. *Nature* **370,** 304–307 (1994).
20. Rancourt, D. E., Tsuzuki, T. & Capecchi, M. R. *Genes Dev.* **9,** 108–122 (1995).
21. Shubin, N. H. & Alberch, P. *Evol. Biol.* **20,** 319–387 (1986).
22. Oster, G. F., Shubin, N., Murray, J. D. & Alberch, P. *Evolution* **42,** 862–884 (1988).
23. Duboule, D. *Science* **266,** 575–576 (1994).
24. Tabin, C. *Cell* **80,** 671–674 (1995).
25. Niswander, L., Tickle, C., Vogel, A., Booth, I. & Martin, G. R. *Cell* **75,** 579–587 (1993).
26. Fallon, J. F. *et al. Science* **264,** 104–107 (1994).
27. Niswander, L., Jeffrey, S., Martin, G. R. & Tickle, C. *Nature* **371,** 609–612 (1994).
28. Cohn, M. J., Izpisúa-Belmonte, J.-C., Abud, H., Heath, J. K. & Tickle, C. *Cell* **80,** 739–746 (1995).
29. Peterson, R. L., Papenbrock, T., Davda, M. M. & Awgulewitsch, A. *Mech. Dev.* **47,** 253–260 (1994).


ACKNOWLEDGEMENTS. A.P.D. was supported by an NSF predoctoral fellowship and an NIH genetics training grant. We thank K. Saalfeld, T. Smith and C. Lewis for technical support, and L. Oswald for help with the preparation of the manuscript.

# Crucial role of the pre-T-cell receptor α gene in development of αβ but not γδ T cells

**Hans Jörg Fehling*, Anna Krotkova*, Claude Saint-Ruf† & Harald von Boehmer***

* Basel Institute for Immunology, CH-4005 Basel, Switzerland
† Institut Necker, Unité INSERM 373, 156 rue de Vaugirard, 75730 Paris Cedex 15, France

**In T-cell precursors, the T-cell-receptor β chain is expressed before the T-cell-receptor α chain[1,2] and is sufficient to advance T-cell development in the absence of T-cell receptor α chains[3–7]. In immature T cells, the T-cell-receptor β protein can form disulphide-linked heterodimers with the pre-T-cell-receptor α chain[8,9] and associate with signal-transducing CD3 molecules[5]. The recently cloned pre-T-cell-receptor α gene encodes a transmembrane protein that is expressed in immature but not mature T cells[9,10]. Here we show that αβ, but not γδ, cell development is severely hampered in pre-T-cell-receptor α-gene-deficient mice, which establishes a crucial role for the pre-T-cell receptor in early thymocyte development.**

Intrathymic T-cell development proceeds from $CD4^-8^-$ precursors through $CD4^+8^+$ intermediates into $CD4^+8^-$ and $CD4^-8^+$ mature thymocytes[3,11]. In rearrangement-deficient mice, thymocyte development is arrested at the $CD4^-8^-3^{low}25^+$ stage[6,7,12]. Productive T-cell-receptor (TCR)-β transgenes can partly relieve the developmental block, allowing the accumulation of immature $CD4^+8^+$ thymocytes but not mature $CD4^+8^-$ and $CD4^-8^+$ T cells[3–7] that require positive selection by TCRαβ (ref. 13). In T-cell precursors the TCR-β chain forms disulphide-linked heterodimers with the pre-TCRα (pTα) chain, and can associate with signal-transducing CD3 molecules[5,8,9].

Here we report on the role of the TCRβ–pTα heterodimer in development, based on experiments with pTα-deficient mice. These animals were generated by gene targeting in embryonic stem (ES) cells using a deletion-type targeting vector. On homologous recombination, this construct eliminated exons 3 and 4 of the pTα gene encoding the connecting peptide, which contains the cysteine required for heterodimer formation, the transmembrane region, the cytoplasmic tail and most of the 3′ untranslated region (Fig. 1). Homologous recombination in ES cells and the absence of the deleted gene segment in $pT\alpha^{-/-}$ mice was verified by Southern blotting with appropriate probes (Fig. 1, and results not shown). Offspring from intercrosses of $pT\alpha^{+/-}$